NATURAL CONVECTION THROUGH ENCLOSED DISCONNECTED SOLID BLOCKS

Fernando César De Lai, fernandodelai@gmail.com
Silvio L. M. Junqueira, silvio@utfpr.edu.br
Admilson T. Franco, admilson@utfpr.edu.br
UTFPR, Curitiba-PR 80230-901, BRAZIL

José L. Lage, JLL@smu.edu
SMU, Dallas-TX 75275-0337, USA

Abstract. *In this study, the natural convection inside a fluid filled, enclosure containing several solid obstructions and being heated from the side is modeled and numerically simulated. The solid obstructions are equally spaced, conducting, and disconnected square blocks. The mathematical model is based on the balance equations of mass, momentum and energy, which are then solved numerically via the finite-volume method with the SIMPLEST algorithm and the HYBRID scheme. The effects of varying the solid-fluid thermal conductivity ratio (K), the fluid volume-fraction or porosity (ϕ), the number of solid blocks (N) and the heating strength (represented by the Rayleigh number, Ra) of the enclosure on the Nusselt number based on the surface-averaged heat transfer coefficient along the heated wall of the enclosure are studied. The results indicate a competing effect caused by the proximity of the solid blocks to the heated and cooled walls, vis-à-vis hindering the boundary layer growth, hence reducing the heat transfer effectiveness, and at the same time enhancing the heat transfer when the blocks' thermal conductivity is larger than that of the fluid. An analytical estimate of the minimum number of blocks beyond which the convection hindrance becomes predominant is presented and validated by the numerical results.*

Keywords*: Natural convection, Enclosure, Porous media, Heat transfer, Porosity.*

1. INTRODUCTION

The study of natural convection in porous cavities has been the focus of several studies along the last few decades. Nield and Bejan (1992) and Whitaker (1999) describe applications of convection in porous cavities in several areas, such as project and system optimization in construction (thermal insulation of building structures and solar heating), in electronics (system packaging), food industry (drying and storage of grains), in biomedical engineering, pollution dispersion, liquid crystal manufacturing, materials processing, gas and oil exploration, where the understanding of the transport phenomena in porous media is vital to the economic interest.

Particularly in oil and gas reservoir drilling and production, the study of heat transfer and percolation includes the determination of velocity, temperature and pressure fields in the non-homogeneous medium (the reservoir), considered a porous medium. These determinations require the knowledge of the thermo-hydraulic characteristics of the medium, where properties such as permeability and porosity are strongly influenced by the geometry of the medium, or more precisely, the interface between the several constituents of the medium.

The heterogeneous model to be followed in this study is based on two constituents, that is, a solid and a fluid (liquid), with balance equations valid for each constituent separately. This model is called "microscopic" or continuum model. Alternatively, a homogeneous model, also called porous-continuum, where conservation equations are developed for the entire medium as if it were homogeneous (following the volume-averaging technique, for instance), is advantageous since the interface characterization of the medium is not needed. On the other hand, the homogeneous model requires thermo-physical properties to be determined, and those are very difficult to find.

One of the first studies focusing on natural convection in fluid filled enclosures partially obstructed by solid blocks was done by House *et al*. (1990). In this work, the effect on natural convection of changes on the thermal conductivity of a single solid block placed at the center of the square enclosure was investigated. A similar geometry, with the block considered adiabatic (nonparticipating), was studied by Bhave *et al*. (2006). In this study, an optimal dimension of the block for maximizing the heat transfer across the enclosure was found. For dimension larger than this optimum dimension the natural convection process inside the enclosure is hindered.

Merrikh and Mohamad (2001) considered the additional effect of energy generation inside the blocks. Their results were confirmed later on by Merrikh and Lage (2005) and Merrikh *et al.* (2005), who compared the continuum-model results (when solid and fluid are modeled separately, in a nonhomogeneous approach) to the porous-continuum model approach (in which fluid and solid blocks are considered a homogeneous, porous medium). In this case, the solid blocks did not generate heat and were placed equally spaced inside the enclosure, uniformly distributed. The comparison between the microscopic (continuum model) and macroscopic (porous-continuum model) approaches was also considered by Braga and de Lemos (2005a), who obtained numerical solutions for the natural convection in laminar and turbulent regimes. Additionally, Braga and de Lemos (2005b) investigated the influence of the blocks geometry on the heat transfer process. Comparing the results for square and circular blocks (both equally distributed), they concluded

that the flow separation caused by the corners of the square blocks are likely responsible for the intensification of the heat transfer process, as compared to the circular blocks case.

The present study is concerned with the study of natural convection in a square enclosure partially filled with solid, thermally conducting, disconnected square blocks. The enclosure is heated laterally. The balance equations ruling the heat transfer and the ensuing fluid flow process are solved numerically by the finite-volume method. The focus is on the effects of varying the fluid-to-solid thermal conductivity ratio, for a fixed fluid volume-fraction value (equivalent to the enclosure porosity) and on changing the volume-fraction of the fluid for a constant fluid-to-solid thermal conductivity ratio.

The results form a useful reference for obtaining synthetic porous media, useful also for the characterization of petroleum reservoirs, as they present the effects of thermal conductivity ratio and porosity on the isotherms and streamlines inside the enclosure.

2. PROBLEM FORMULATION

Figure 1, which presents the heterogeneous domain being investigated, shows the disconnected, solid square blocks uniformly distributed inside the fluid filled enclosure. The enclosure is heated horizontally (isothermally heated left wall and cooled right wall), with adiabatic top and bottom surfaces.

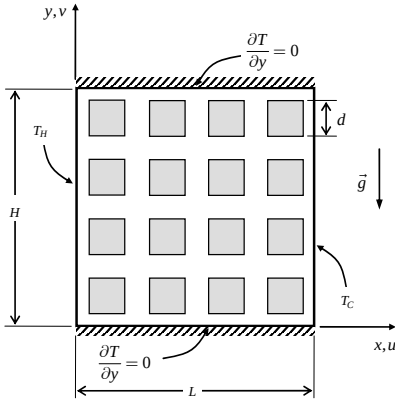

Figure 1. Heterogeneous domain (continuum approach) with boundary conditions.

2.1. Governing equations and boundary conditions

Considering steady-state, and constant and uniform properties of a Newtonian fluid, the conservation equations of mass (continuity), momentum (in the horizontal and vertical directions) and energy are:

$$\frac{\partial u}{\partial x}+\frac{\partial \upsilon}{\partial y}=0 \tag{1}$$

$$u\frac{\partial u}{\partial x}+\upsilon\frac{\partial u}{\partial y}=-\frac{1}{\rho_f}\frac{\partial p}{\partial x}+\nu\nabla^2 u \tag{2}$$

$$u\frac{\partial \upsilon}{\partial x}+\upsilon\frac{\partial \upsilon}{\partial y}=-\frac{1}{\rho_f}\frac{\partial p}{\partial y}+\nu\nabla^2 \upsilon+g\beta\left(T-T_{ref}\right) \tag{3}$$

$$u\frac{\partial T}{\partial x}+\upsilon\frac{\partial T}{\partial y}=\alpha_f\left(\frac{\partial^2 T}{\partial x^2}+\frac{\partial^2 T}{\partial y^2}\right) \tag{4}$$

where u e υ are the velocity components in the x and y directions, respectively; p is the pressure, ρ_f is the fluid density, ν is the fluid kinematic viscosity, g is the acceleration of gravity, β is the isobaric coefficient of volumetric thermal expansion and α_f is the thermal diffusivity of the fluid. Observe that the Oberbeck-Boussinesq (Bejan, 1995) approximation is invoked for modeling the body-force term of the vertical momentum equation, where T_{ref} the fluid reference temperature, usually considered equal to the lowest temperature in the enclosure, T_C.

For the solid blocks, considered homogeneous and isotropic, the steady-state heat transfer equation is:

$$k_s \nabla^2 T = 0 \tag{5}$$

where k_s é is the thermal conductivity of the solid block.

In the enclosure presented in Figure 1, the velocity components u and υ are considered zero along the solid boundaries of the enclosure. The left and right walls of the enclosure are kept, respectively, at T_H and T_C.

Equations (1)-(5) have been nondimensionalized using the following parameters: $(X,Y) = (x,y)/H$, where H is the enclosure height (same as width), $(U,V) = (u,v)/(\alpha_f / H)$, $P = pH^2 / \rho_f(\alpha_f)^2$ and $\theta = (T - T_C)/(T_H - T_C)$. The resulting equations for the fluid are:

$$\frac{\partial U}{\partial X} + \frac{\partial V}{\partial Y} = 0 \tag{6}$$

$$U\frac{\partial U}{\partial X} + V\frac{\partial U}{\partial Y} = -\frac{\partial P}{\partial X} + Pr\left(\frac{\partial^2 U}{\partial X^2} + \frac{\partial^2 U}{\partial Y^2}\right) \tag{7}$$

$$U\frac{\partial V}{\partial X} + V\frac{\partial V}{\partial Y} = -\frac{\partial P}{\partial Y} + Pr\left(\frac{\partial^2 V}{\partial X^2} + \frac{\partial^2 V}{\partial Y^2}\right) + Ra\,Pr\,\theta \tag{8}$$

$$\left(\frac{K}{\sigma}\right)\left(U\frac{\partial \theta}{\partial X} + V\frac{\partial \theta}{\partial Y}\right) = \frac{\partial^2 \theta}{\partial X^2} + \frac{\partial^2 \theta}{\partial Y^2} \tag{9}$$

and for the solid blocks:

$$\nabla^2 \theta = 0 \tag{10}$$

In equation (6)-(10), the nondimensional parameters are $Pr = \nu/\alpha_f$ as the Prandtl number, $Ra = g\beta H^3 (T_H - T_C)/\nu\alpha_f$ as the Rayleigh number, $\sigma = (\rho c)_s / (\rho c)_f$, as the solid-fluid thermal capacity and $K = k_s / k_f$ as the solid-fluid thermal conductivity ratio.

The nondimensional representation of the boundary conditions:

for $X = 0$: $U = V = 0$, $\theta = 1$; (11)

for $X = 1$: $U = V = 0$, $\theta = 0$; (12)

for $Y = 0$ e $Y = 1$: $\dfrac{\partial \theta}{\partial Y} = U = V = 0$; (13)

$$U = V = 0;\ \theta\big|_f = \theta\big|_s;\ \frac{\partial \theta}{\partial n}\bigg|_f = K\frac{\partial \theta}{\partial n}\bigg|_s;\ \frac{\partial \psi}{\partial n}\bigg|_f = \frac{\partial \psi}{\partial n}\bigg|_s, \tag{14}$$

where n is the unit vector normal to each block surface and ψ is the stream function, defined in Eq. (15), which according to Kimura e Bejan (1983), can be physically unified to satisfy the continuity equation (6).

$$\psi = \int_0^1 U dY = -\int_0^1 V dX \tag{15}$$

Keep in mind the compatibility conditions of nonslip and continuous heat flux are imposed along the surfaces of each solid block.

The heat transfer characteristics inside the enclosure are better established using the surface-averaged Nusselt, defined as $Nu_{av} = h_{av} H / k_f$, where the average heat transfer coefficient, h_{av}, is obtained through its definition $h_{av} = q''_{av} / (T_H - T_C)$, where the heat flux is determined along the hot wall $q''_{av} = -k_f (\partial T / \partial x)_{av,h}$. Hence, the hot wall-averaged Nusselt number, which is identical to the Nusselt number of the cold wall, becomes:

$$Nu_{av} = \frac{h_{av} H}{k_f} = -\int_0^1 \left.\frac{\partial \theta}{\partial X}\right|_{X=0} dY \tag{16}$$

In summary, the continuum model results depend on the following parameters: *Ra*, *Pr*, σ , *K* and on the geometric parameters *A*, *D* e *N*, which are respectively, the aspect ratio of the enclosure, $A = L / H$, the dimensional side-length of the blocks, $D = d / H$, and the total number of blocks inside the enclosure, *N*.

3. RESULTS AND DISCUSSION

The conservation equations (6)-(10) were solved using the finite-volume method, with a hybrid scheme for the convective terms (Patankar,1980), with the SIMPLEST algorithm (Patankar,1981 and Versteeg and Malalasekera,1995). Convergence was determined using the residual control criterion of Spalding (1994), setting a maximum of 10^{-6} for the sum of all absolute residuals of *U*, *V*, *P* and θ below which the solution is considered converged.

In the present study, *A* = *Pr* = 1. The number of blocks *N* varied from 9 to 144, and the Rayleigh *Ra* from 10^5 to 10^8. The solid-fluid thermal conductivity ratio *K* is varied from 0.1 to 100, for porosity ϕ = 0.64. Similarly, to isolate the porosity effect, the porosity ϕ is varied from 0.36 to 0.84, for the case *K* = 1. Observe these configurations are established by finding the value of *D* to satisfy the set values of *N* and ϕ , using the equation $D = [(1-\phi) / N]^{0.5}$, where $(1-\phi)$ represents the solid volume-fraction inside the enclosure. For the cases of varying *K* the porosity is maintained constant by decreasing the value of *D* as the number of blocks *N* increases. On the other hand, for the study of varying ϕ , besides a constant *K*, the value of *D* has to be decreased in accordance to the increase in ϕ for each number of blocks *N*. A summary of the parameter values used in this study is presented in Table 1.

Table 1. Summary of parameter values.

Ra	10^5, 10^6, 10^7, 10^8
N	9, 16, 36, 64, 144
K	0.1, 1, 10, 100
ϕ	0.36, 0.51, 0.64, 0.75, 0.84

Table 2 presents a comparison between the present simulations and results available in the literature for similar configurations. The good comparison gives credence to the results obtained here. The results are for an enclosure clear of solid blocks. Observe the results were obtained using 320 by 320 grid points, distributed uniformly within the enclosure. Grid accuracy tests were performed for different values of Rayleigh number (see Table 3), with the relative percentage error being small, even when the Rayleigh number is high, as the number of grid points increased from 160 to 320.

For the configuration with solid blocks inside the enclosure, the grid accuracy test results, presented in Table 4, were obtained for the most restrictive configurations, namely *Ra* = 10^8, *N* = 144, *K* = 0.1, and ϕ = 0.64, and for ϕ = 0.36 and *K* = 1. Notice the relative percent error for grids 241 and 481 was also small, hence the results were obtained with a 481×481 grid.

Table 2. Comparison with published results based on the wall-averaged Nusselt number.

Ra	House *et al.* (1990)	de Vahl Davis (1983)	Hortmann *et al.* (1990)	Kalita *et al.* (2001)	[present]	Lage and Bejan (1991)	Lage and Merrikh (2005)	Braga and de Lemos (2005a)	[present]
	Pr = 0.71	*Pr* = 0.71	*Pr* = 0.71	*Pr* = 0.71	*Pr* = 0.71	*Pr* = 1	*Pr* = 1	*Pr* = 1	*Pr* = 1
10^4	2.254	2.243	2.244	2.245	2.245	-	2.244	2.249	2.257
10^5	4.561	4.519	4.521	4.522	4.523	4.900	4.536	4.575	4.602
10^6	8.923	8.800	8.825	8.829	8.835	9.200	8.860	8.918	8.991
10^7	-	-	-	16.520	16.582	17.900	16.625	16.725	16.928
10^8	-	-	-	-	30.444	31.800	31.200	30.642	31.386

Table 3. Grid accuracy test results for enclosure without blocks.

Ra	Nu_{av} Malha 160×160	Nu_{av} Malha 320×320	*EP*
10^4	2.246	2.245	0.035
10^5	4.528	4.523	0.111
10^6	8.865	8.835	0.340
10^7	16.752	16.582	1.020
10^8	31.483	30.444	3.415

Table 4. Grid accuracy test results for most stringent configurations.

Ra	*N*	*K*	ϕ	Nu_{av} 241×241	Nu_{av} 481×481	*EP*
10^8	144	0.1	0.64	21.280	20.111	5.814
10^8	144	1	0.36	6.294	5.663	11.147

The geometrical effect of placing blocks with different sizes and in different numbers inside the enclosure can be considered via the distance the first column of blocks has from the walls of the enclosure. The heat transfer process evolves, and the fluid begins its buoyancy induced movement, a boundary layer forms along the hot (left) wall and the cold (right) wall of the enclosure. If the blocks are placed too close to the walls, that is, inside the region which would otherwise be occupied by the boundary layers, the solid surface of the blocks would affect the flow, hindering its development by friction effect. Hence, it is conceivable that a minimum number of blocks, referred to as N_{min}, exists beyond which the blocks affect the flow in a more pronounced way. Observe that the growth of the boundary layer along the hot and cold walls is affected by the Rayleigh number being considered. An estimate for when the boundary layer thickness for natural convection between two parallel walls, for $Pr \geq 1$ and only one heated wall, Bejan (1995), matches the distance *S* between the two walls is $Ra^{-1/4} \sim S/2$, where *S* in the present case would represent the distance between the enclosure wall and the sides of the row of blocks adjacent to it. Using the relation between *S* and *A*, a criterion for a minimum number of blocks is obtained as

$$N > \frac{[1-(1-\phi)^{1/2}]^2}{16} Ra^{1/2} \tag{17}$$

So, when *N* is bigger than N_{min} the presence of solid blocks is likely to affect the flow along the walls. Results from Eq. (17) are shown in Table 5. Observe that for small *Ra* the minimum number of blocks is quite small, increasing as Ra increases. When *Ra* is very high, for instance $Ra = 10^8$, the minimum number of blocks becomes very high (over 60 blocks) for *f* greater than 0.51.

Table 5. Predicted N_{min} for boundary layer interference.

Ra	ϕ				
	0.36	0.51	0.64	0.75	0.84
10^5	1	2	3	5	7
10^6	3	6	10	16	23
10^7	8	18	32	49	71
10^8	25	56	100	156	225

In relation to the natural convection process inside the enclosure, numerical results shown in Table 6 indicate that an increase in the number of blocks *N* usually yields a decrease in the Nusselt number for the same Rayleigh number and porosity values. This observation is in line with the minimum number of blocks results of Table 5. Observe further that for $Ra = 10^8$ and porosity 0.84, the Nusselt value does not change much as *N* increases, decreasing *Nu* only when *N* goes beyond 64, a result qualitatively in line with the predicted N_{min} in Table 5.

Additionally, an extension of the study by Merrikh and Lage (2005) involves the effect of varying the porosity of the enclosure. Table 6 shows Nu_{av} for $Ra = 10^7$ e 10^8, considering $K = 1$, and several porosity ϕ values. From it, one can see that as *f* increases so does Nu_{av} as expected because larger porosity means less restriction by solid blocks. Interestingly, and perhaps less expected, is the intensity of the porosity increase effect. When the number of blocks in the enclosure is small, say for instance when *N* is less than 36, the porosity increase initially leads to a large increase in

the Nusselt number, but after a certain porosity value the Nusselt number plateaus and it does not increase as much anymore. That is, the porosity effect becomes much less evident.

Table 6. Average Nusselt number for $K = 1$.

Ra	*N*	ϕ				
		0.36	0.51	0.64	0.75	0.84
10^7	9	**9.551**	14.600	16.126	16.658	16.885
	16	**5.807**	**12.450**	**15.320**	15.258	16.642
	36	3.020	**7.049**	**12.039**	**14.903**	16.168
	64	2.426	4.165	8.089	**11.135**	**14.503**
	144	1.850	3.422	5.291	7.562	**10.052**
10^8	9	27.987	30.284	30.866	30.973	30.974
	16	**25.610**	29.477	30.429	29.855	31.006
	36	**17.421**	**27.380**	29.890	30.416	30.696
	64	9.811	**22.111**	**28.291**	28.328	30.650
	144	5.663	11.683	**20.064**	26.234	29.239

Figure 2 shows streamlines and isotherms for ϕ = 0.36, 0.64 and 0.84, and $Ra = 10^6$, $N = 36$ e $K = 1$. For these configurations it is possible to observe that the increase in f affects the flow inside the enclosure, with more fluid flowing more strongly along the heated and cooled walls. This aspect is easily seen in the isotherm distribution where the stratified core of the enclosure is observable – this isotherm distribution resembles that seen for the case of an enclosure without any solid blocks. The corresponding increase in Nusselt number is a consequence of this flow behavior. Observe from Table 5 that the minimum number of blocks for each porosity in this case is respectively 3, 10, and 23, that is less than the 36 used. Hence, one would not expect a strong effect of the blocks on the boundary layers along the hot and cold walls. In fact, here the effect in opposite: the increase in porosity provides more area for the fluid to flow along the hot and cold walls, enhancing the heat transfer process.

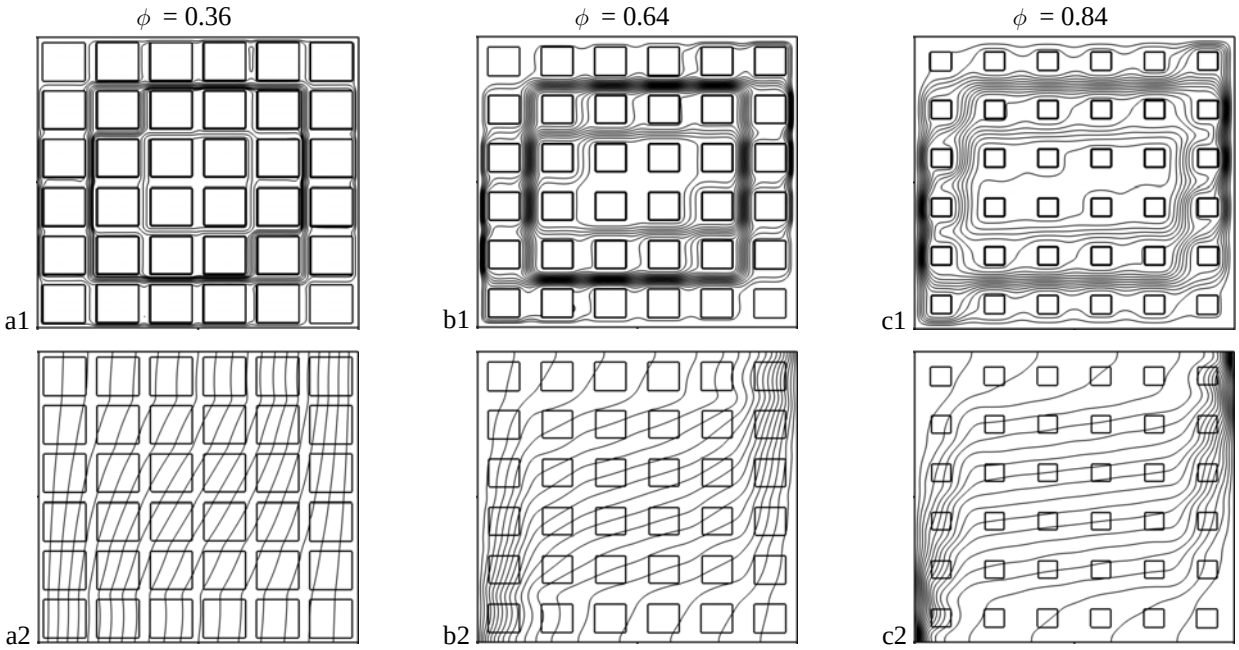

Figure 2. (a1), (b1) e (c1) Streamlines; (a2), (b2) e (c2) isotherms for $Ra = 10^6$, $N = 36$ and $K = 1$.

Results presented by Merrikh and Lage (2005) indicate that the reduction in Nu_{av} due to the block proximity to the hot and cold wall boundary layers is stronger for low *Ra*. According to Figure 3, it is possible to observe that the Nu_{av} reduction takes place at different *Ra* values for each ϕ. Here, the *Ra* values, for each ϕ, presenting the strongest reduction in Nu_{av} with an increase in *N* from 9 to 144, are: i) $Ra = 10^7$ for ϕ = 0.36 and 0.51 e ii) $Ra = 10^6$ for ϕ = 0.64,

0.75 and 0.84. Considering now the ϕ values for each *Ra*, the configurations for the strongest Nu_{av} reduction are: i) ϕ = 0.84 for $Ra = 10^5$; ii) ϕ = 0.64 for $Ra = 10^6$ and iii) ϕ = 0.36 for $Ra = 10^7$ and 10^8. The strongest reduction in Nu_{av} occurs when ϕ = 0.36 and $Ra = 10^7$, with Nu_{av} obtained when N = 9 decreasing by more than five times to the value of Nu_{av} when N = 144.

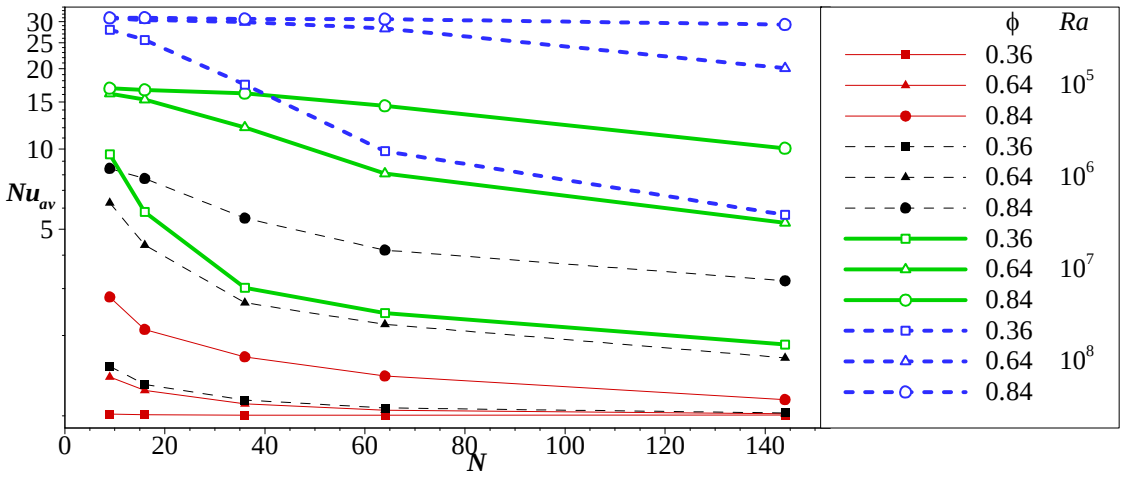

Figure 3. Average Nusselt number versus number of blocks, for K = 1.

The solid-fluid thermal conductivity ratio K effect is considered in line with the results presented in Table 7. Observe that the results obtained here for K = 0.1, 1, 10 and 100, *Ra* from 10^5 to 10^8 and N from 9 to 144 and for ϕ = 0.64, were compared against the results published by Merrikh and Lage (2005), with a discrepancy of less than 1.2%. From Table 7, it is seen that for a fixed *Ra*, that Nu_{av} decreases as K increases when N is small. For large N, the K effect switches to increasing Nu_{av}. This behavior can be understood considering the effect of having a high thermal conductivity solid near the heated or cooled walls. If the blocks are placed very closed to the walls, their presence would tend to hinder the natural convection along the hot or cold walls, but it would also help transfer the heat within the enclosure (because heat would conduct better through the high thermal conductivity blocks than through the stagnant fluid). In Table 6, this phenomenon is observable for $Ra = 10^6$ when N = 16 for K = 1 and 10. For $Ra = 10^7$, on the other hand, the switch takes place for N = 36 when K varies from 10 to 100.

Table 7. Average Nusselt number for ϕ = 0.64.

Ra	*N*	*K*			
		0.1	1	10	100
10^6	9	6.658	6.283	5.927	5.914
	16	4.577	**4.365**	**4.637**	4.861
	36	2.137	2.654	3.635	3.947
	64	1.597	2.203	3.074	3.341
	144	1.206	1.649	2.381	2.633
10^7	9	16.299	16.126	15.719	15.542
	16	15.542	15.320	14.808	14.599
	36	12.433	12.039	**11.699**	**11.726**
	64	7.927	8.089	9.141	9.628
	144	4.103	5.291	7.188	7.740

4. SUMMARY AND CONCLUSIONS

The natural convection inside a fluid filled enclosure with conducting, equally spaced, disconnected solid blocks is considered here. Results are obtained for several different configurations focusing on the solid-to-fluid thermal conductivity ratio effect and on the porosity effect. The proximity of the blocks to the heated and cooled walls of the enclosure affects the heat transport in two competing ways. Firstly, when the blocks are close to the walls they can eventually interfere with the boundary layers, hindering the flow. This effect is anticipated on the basis of a scale

analysis result predicting the boundary layer thickness. Secondly, when the thermal conductivity of the blocks is larger than the thermal conductivity of the fluid, the proximity of the blocks to the heated and cooled walls can help the heat transfer across the enclosure, enhancing the convective effect. In general, increasing the porosity enhances the heat transfer process, increasing the Nusselt number. These considerations help explain the very different shape of the Nusselt number curves versus the number of blocks in the enclosure as the Rayleigh number changes.

4. ACKNOWLEDGEMENTS

The first three authors are grateful to the financial support provided by the Brazilian Petroleum Agency (ANP) by the Human Resources Program for the Petroleum and Gas Sector PRH-ANP (PRH10 – UTFPR) and CENPES-PETROBRAS.

5. REFERENCES

Bejan, A., 1995, Convection Heat Transfer, second ed., John Wiley & Sons Inc.

Bhave, P., Narasimhan, A. and Rees, D.A.S., 2006, "Natural convection heat transfer enhancement using adiabatic block: Optimal block size and Prandtl number effect", International Journal of Heat and Mass Transfer Vol.49, pp. 3807-3818.

Braga, E.J. and de Lemos, M.J.S., 2005a, "Heat transfer in enclosures having a fixed amount of solid material simulated with heterogeneous and homogeneous models", International Journal of Heat and Mass Transfer Vol.48, pp. 4748-4765.

Braga, E.J. and de Lemos, M.J.S., 2005b, "Laminar natural convection in cavities filled with circular and square rods", International Communications in Heat and Mass Transfer Vol.32, pp. 1289-1297.

Hortmann, M., Peric, M. and Scheuerer G., 1990, "Finite volume multigrid prediction of laminar natural convection: benchmark solutions", International Journal of Numerical Methods Fluids Vol.11, pp. 189-207.

House, J.M., Beckermann, C. and Smith T.F., 1990, "Effect of a centered conducting body on natural convection heat transfer in an enclosure", Numerical Heat Transfer, Part A Vol.18, pp. 213-225.

Kalita, J.C., Dalal, D.C. and Dass, A.K., 2001, "Fully compact higher order computation of steady-state natural convection in a square cavity", Phys. Rev. E64 (066703), pp. 1-13.

Kimura, S. and Bejan, A., 1983, "The 'heatline' visualization of convective heat transfer", ASME J. Heat Transfer Vol.105, pp. 916–919.

Lage, J.L. and Bejan, A., 1991, "The Ra–Pr domain of laminar natural convection in an enclosure heated from the side", Numerical Heat Transfer, Part A Vol.19, pp. 21-41.

Merrikh, A.A. and Lage, J.L., 2005, "Natural convection in an enclosure with disconnected and conducting solid blocks", International Journal of Heat and Mass Transfer Vol.48, pp. 1361-1372.

Merrikh, A. A., Lage, J. L. and Mohamad, A. A., 2005, "Natural Convection in Non-homogeneous Heat-Generating Media: Comparison of Continuum and Porous-Continuum Models", Journal Porous Media, Vol.8, pp. 149-163.

Merrikh, A. A. and Mohamad, A. A., 2001, "Blockage effects in natural convection in differentially heated enclosure", Journal Enhanced Heat Transfer Vol.8, pp. 55-74.

Nield, D.A. and Bejan, A., 1992, Convection in Porous Media, Springer, New York.

Patankar, S.V., 1981, "A Calculation Procedure for Two-dimensional Elliptic Situations", Numerical Heat Transfer, Vol.4, pp. 409-425.

Patankar, S.V., 1980, "Numerical Heat Transfer and Fluid Flow", Hemisphere Publishing, New York, 1980.

PHOENICS, 1991, Reference Manual, Part A: PIL. TR 200 A, Bakery House, London SW 19 5AU, UK: Concentration Heat and Momentum Limited.

Spalding, D.B., 1994, The PHOENICS Encyclopedia, CHAM Ltda, London, UK.

Vahl Davis, G., 1983, "Natural convection of air in a square cavity: a bench mark numerical solution", International Journal of Numerical Methods Fluids Vol.3, pp. 249-264.

Versteeg, H.K. and Malalasekera, W., 1995, "An Introduction to Computational Fluid Dynamics", Harlow, UK: Longman Group Ltd.

Whitaker, S., 1999, "Theory and applications of transport in porous media: The method of volume averaging", Kluwer Academic Publishers, 101 Philip Drive, Norwell, U.S.A.

6. RESPONSIBILITY NOTICE

The authors are the only responsible for the printed material included in this paper.